Available online at www.sciencedirect.com
ScienceDirect
International Journal of Pharmaceutics 328 (2007) 78–85
INTERNATIONAL JOURNAL OF PHARMACEUTICS
www.elsevier.com/locate/ijpharm

Pharmaceutical Nanotechnology

PVP magnetic nanospheres: Biocompatibility, in vitro and in vivo bleomycin release

Ding Guowei [a,*], Kamulegeya Adriane [b], XingZai Chen [c], Chen Jie [d], Liu Yinfeng [e]

[a] *Tongji university hospital, 50 Chifeng Road, 200092 Shanghai, PR China*
[b] *Department of oral and maxillofacial surgery, Tongji stomatological hospital, PR China*
[c] *Affiliated hospital of Taian medical college, Shangdong, PR China*
[d] *Department of Chemical Engineering and Technology, Shanghai University Shanghai 201800, China*
[e] *Department of Polymer Materials, Shanghai University, China*

Received 8 February 2006; received in revised form 11 May 2006; accepted 25 July 2006
Available online 4 August 2006

Abstract

Purpose: To synthesize and characterize a magnetic micromolecular delivery system based on PVP hydrogel with polyvinyl alcohol (PVA) as the crosslinker.
Methods: The microparticles were successfully prepared using 25 kGy Co-60 γ-ray irradiation and characterized. Biocompatibility, in vitro and in vivo drug release tests were carried out.
Results and discussion: Bleomycin was quantitatively released with in slightly over 8 h (hours) from the nanospheres containing 1 mg bleomycin while the time was longer for those containing 5 mg. On the other hand free bleomycin quantitatively passed through the dialysis baffle with in only 3.5 h. For both 5 and 1 mg of bound bleomycin, it took up to 2 h to reach peak concentration compared to 30 min for the free drug.
Conclusion: The PVP hydrogel magnetic nanospheres exhibited passive drug release that could be exploited to enhance therapeutic efficacy. The present results indicate that PVP hydrogel based magnetic nanospheres have potential as drug carriers in magnetic guided chemotherapeutic drug delivery.

Keywords: Polyvinylpyrrolidone (PVP) hydrogel; Nanospheres; Magnetic micromolecules; Magnetic guided drug delivery

1. Introduction

Chemotherapeutic drugs are extensively used in oncology treatment regimens. However, due to their lack of specificity, they cause untoward cytotoxic effects to the patients hence limiting their usefulness. To circumvent this problem, a lot of modalities have been developed aiming mainly at achieving high therapeutic efficacy while keeping cytotoxicity to a minimum. These modalities include; chemotherapeutic prodrugs activated at tumor site, tagged drugs, combination therapy (such as chemotherapy with immunotherapy, vascular targeting, and interventional genetics), and magnetic drug guidance, etc. (Youssef and David, 2000; Kupsch et al., 2005; Gurnani et al., 1999; Lubbe et al., 2001; Häfeli, 2004).

Magnetic guided drug delivery has seen enormous development with different carriers proposed such as polybutylcyanoacrylate, starch based polymers, oleic acid (AO) pluronic acid, liposome, dextran, and iron activated carbon microparticles. All these systems are aimed at minimizing carrier uptake by the reticuloendothelial system. To further improve efficacy and reduce reticuloendothelial system uptake, the carriers are given locoregionaly by itraarterial or intratumoral routes of administration with a magnet in place to draw and retain the carriers at the tumor site (Gao et al., 2004; Christoph et al., 2000; Tapan et al., 2005; Hiroo et al., 2004; Cheung et al., 2005; Rudge et al., 2001). Magnetic drug targeting has been applied in both experimental and clinical cancer therapy. Lubbe et al. (1996a,b) published their preclinical results of magnetic drug targeting using epirubicin bound ferrofluid in experimental human kidney tumors and xenotransplanted colon cancer models. In the same journal issue, Lubbe et al. (1996a,b) also reported having successfully directed epirubicin in increasing doses (from 5 to 100 mg/m^2)

* Corresponding author. Tel.: +86 21 65988382; fax: +86 21 65988385.
E-mail address: tjhosp698@sohu.com (D. Guowei).

0378-5173/$ – see front matter © 2006 Elsevier B.V. All rights reserved.
doi:10.1016/j.ijpharm.2006.07.042

chemically bound to a magnetic fluid to tumors in about one-half of patients with advanced solid tumors. Christoph et al. (2000) also reported successfully treating implanted VX2 rabbit squamous cell carcinoma by concentrating ferrofluid bound-MTX in tumor tissue using an external magnetic field. With the intention of contributing to the growing array of magnetic guided carrier systems, we set out to synthesize a polyvinylpyrrolidone (PVP) hydrogel based magnetic micromolecular chemotherapeutic drug delivery system. The choice of PVP was due to its long-standing and safe record in biomedical/pharmaceutical application. Additionally it has been reported to enhance drug circulatory time in plasma when used as delivery system (Volker, 2004; Robinson et al., 1990; Kaneda et al., 2004.)

PVP based hydrogels have been used in research and clinical setting as delivery systems with good results reported (Jana et al., 2002; Reimer et al., 1997; Risbud et al., 2000). The properties exhibited by these PVP based hydrogels and the known supraparamagnetic properties of iron oxide formed the basis of our research to synthesize magnetic micromolecular delivery system based on PVP hydrogel with polyvinyl alcohol (PVA) as the crosslinker.

The microparticles were successfully prepared using gamma ray irradiation and characterized. Biocompatibility, in vitro and in vivo drug release tests were carried out.

2. Materials and methods

2.1. Nanosphere synthesis and characterization

The ferrofluid was made using reagent grade polyvinylpyrrolidone (PVP K-30) purchased from BASF (Germany). Other chemicals used were analytical grade purchased from Shanghai Reagent Company and were used as supplied.

Briefly the magnetic hydrogel microspheres were synthesized by irradiating the PVP/PVA and ferro magnetic particles emulsion under constant motion using 25 kGy Co-60 γ-rays with *n*-heptane and 5% (w/w) Span 80 (Sorbitan Mono Oleate) acting as the emulsifying agent. The water phase comprised of 10% weight for weight (w/w) PVP, 2% PVA and about 20% (w/w) ferric oxide. Reverse emulsion was obtained by dropping the water phase into oil phase at a higher stirring speed. Stirring was continued for up to 30 min. After irradiation the oil phase was removed using acetone, water and ethanol. The procedure of synthesis was a modified version as that already described by Müler et al. (1996). The morphology of the nanospheres was observed by a transmission electron microscope TEM (H800 HITACH) and average particle size was determined from several pictures taken with a Quanta 200 ESEM FEG from FEI. The pictures and measurements were done using XT Docu a default image capture and manipulation software of the Quanta 200 ESEM FEG.

With the help of a TG-DTA/DSC apparatus (STA409 PC, NETCH), the composition of the nanospheres was determined. Ten milligrams of the dry nanospheres sample was placed in an aluminum oxide pan and heated from 20 to 400 °C at a rate of 6 °C/min. A nitrogen purge through the sample chamber was used to obtain a more uniform and stable thermal environment. The un-immobilized ferric oxide was removed by socking the sample in 10% aqueous solution of hydrochloric acid before determining its ratio.

2.2. Biocompatibility studies

2.2.1. MTT assay

MTT assay was used as a measure of relative cell viability in contact with nanopheres extract solution. The extracts were obtained by culturing the samples in DMEM with 10% FCS and 1% streptomycin plus penicillin at 37 °C under constant rocking (60 rpm) for 24 h. The extraction was done as per recommendation in ISO document 10993 (1992) with a slight modification to cater for the absorption of DMEM by the nanospheres. DMEM was added to the weighed nanospheres until they could absorb no more. The unabsorbed DMEM was quantified and was taken into consideration during titration to get to the ISO recommended extraction concentration. After 24 h the extracts were filtered using a 0.22 μm filter to eliminate the material but also as a form of sterilization. The MTT tests were handled in just about the same manner as by Müller, R.H et al. The MTT test was done after 24 and 72 h respectively and the reading done at 492 nm using ELISA reader (Bioreader 450). Free DMEM acted as the negative control while latex was the positive control. The cell viability index in percentage was calculated as follows: cell viability index% = (mean absorbency of experimental group at specific extract concentration − mean absorbency of negative control)/(mean absorbency of positive control − mean absorbency of negative control) expressed as a percentage.

2.3. Acute toxicity tests

2.3.1. Experimental animals and conditions

Three weeks old 20–30 gs pathogen free male and female BALB/c rats were purchased from the Tongji University laboratory animal centre and allowed to acclimatize for 1 week before tests. They were fed on standard rat pellet chow (protein 25%, fat 10%, crude fiber 50%, calcium 1.0%, phosphate 0.8% a product of Jiangsu Laboratory Animal Feeds Factory, Nanjing, China) and tap water ad libitum. Five animals per plastic rat cage with chip beddings were maintained in a room at 24 ± 1 °C and 55 ± 5% humidity with a 12 h dark/12 h light cycle.

2.3.2. Experimental design and performance

Groups of five mice were injected with material extracts. The injection was done intravenously through the tail vein for those receiving extract prepared with normal saline while the extract obtained using vegetable oil was given intraperitonealy through the abdominal wall both at a dose of 50 ml/kg. We also had controls injected with normal saline and free vegetable oil using the same dosage and procedure. The rats were monitored for toxic signs such as convulsions, mortality and weight loss/gain immediately, 4, 12, 24, 48, 72 h and up to 4 weeks.

2.4. Hemolytic tests

The hemolytic tests were done as per Anand et al. (2003). In brief, whole rabbit blood from New Zealand white rabbits

(NZW) was drawn from the auricular vessels and immediately added into heparinized tubes. It was used with in 1 h of sampling. The blood was diluted using normal saline so that 0.2 ml of diluted blood would be hemolyzed by 10 ml of distilled water. Spectrometric reading was done at 546 nm. This established a standard baseline. The same dilution was used for test and controls. Distilled water was used as a positive control while normal saline was used as a negative one with 10 ml of each added to the respective vials. All vials in triplicate were incubated at $37 \pm 2\,^{\circ}C$ for 1 h. After incubation they were centrifuged at $500 \times g$ for 5 min. Absorbencies (Abs) of the supernatants were obtained using a UNICO UV 2102 spectrometer. The hemolytic index was calculated as follows.

Hemolytic index% = (mean Abs test article − mean Abs negative control)/(mean Abs positive control − mean Abs negative control) expressed as percentage.

2.5. In vitro drug release

Bleomycin A5 hydrochloride (BLM) was purchased from Harbin Bolai pharmaceutical company (Harbin PRC). It was dissolved in normal saline for use in evaluating the drug release properties of the ferrofluid. First 2.0 mg of bleomycin powder was dissolved in normal saline and then diluted to obtain 2, 4, 8, 16 μg/ml concentrations. Using a grating spectrometer (Shanghai precision scientific instrument company Ltd.) the absorbency of the above concentrations were obtained at 291 nm with saline as the blank. These were used to establish a standard curve shown in Fig. 1. The tests were carried out at $37 \pm 1\,^{\circ}C$, pH 7.4 ± 0.2.

Fifty milligrams dry PVP nanospheres were pre-swelled in 1 ml drug containing solutions with varying concentrations (1, 3 or 5 mg/ml), and sonicated for 30 min to allow for nanosphere separation and improve absorption. After 12 h storage under constant shaking (64 rpm), we supposed the entire drug had been immobilized since no obvious liquid was seen. The drug containing ferrofluid was dispersed by adding 1 ml normal saline and then was injected into 50 ml normal saline in a test device

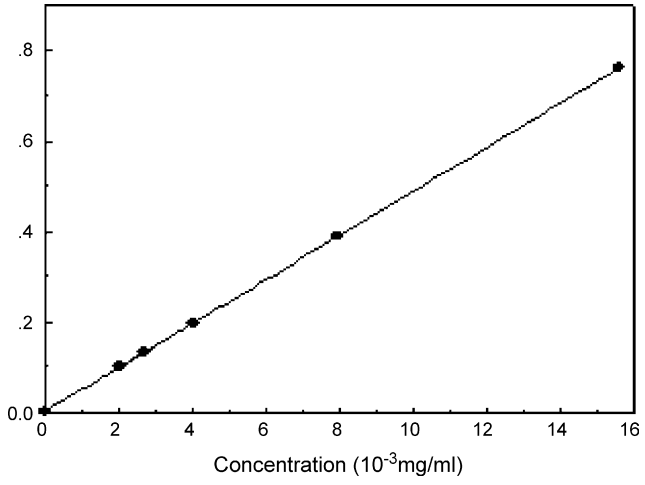

Fig. 1. Bleomycin standard curve obtained using a grating spectrometer.

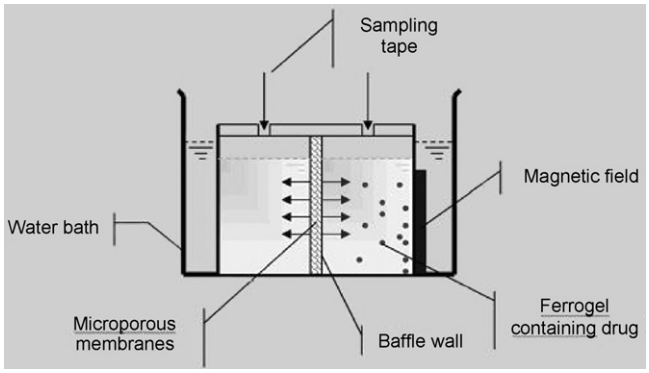

Fig. 2. Schematic diagram of the device for in vitro drug release testing.

designed by Professor Chen Jie (shown in Fig. 2) within a water bath at $37 \pm 1\,^{\circ}C$. The device had a 0.22 μm pore size dialysis wall to keep the free normal saline from the ferrofluid/drug containing saline but yet allow for free drug exchange. It also had a magnet on the test side to attract the nanospheres away from the dialysis baffle. Five milliliters normal saline in the device on the side with out the ferrofluid/drug complex was withdrawn with replenishment every 5 min and used to determine the drug release properties. For comparison, the same amount of drug was injected in the 50 ml normal saline in the test device directly and same procedure was repeated. The drug concentration was determined by absorbance using an UV–vis spectrophotometer (Angilent 100, USA) at 291 nm.

2.6. In vivo drug release

2.6.1. Surgical procedure and sample collection

New Zealand white rabbits with successfully implanted VX2 auricular cancers were used for in vivo drug release monitoring following intraarterial chemoembolization in the presence of a 0.5 T magnet during and after ferrofluid infusion. The VX2 tumors had to have attained a minimum of 200 mm^2 to be considered successful. The tumorous ear blood vessels and the contralateral femoral blood vessels were surgically exposed and lignocaine with adrenaline applied. The auricular central artery and contralateral femoral vein were then cannulated with a 0.7 mm internal diameter scalp cannular (Suzhou BD Company China). With a magnet fixed over the tumor, the ferrofluid containing the drug was slowly infused taking up to 10 min per rabbit. After the infusion, 2 ml of blood were withdrawn from the femoral vein after 30, 60, 180, 360, and 480 min post infusion and put in heparinized vials. The animals were given appropriate anaesthesia and treated in the most humane way possible. After collection, the blood was centrifuged at $3000 \times g$ for 5 min and serum obtained. The serum was stored at $-20\,^{\circ}C$ until analysis. The tissue samples including tumor, ipsilateral lymph nodes, lungs and liver were collected after 8 h post infusion. The animals were euthenized by injection of air into the untreated ear veins and then dissected. Three samples per rabbit, each weighing 0.5 mg were obtained from tissue organs of interest and drug extraction was a slight modification as that done by Yong et al. (2005). Blood samples of appropriate con-

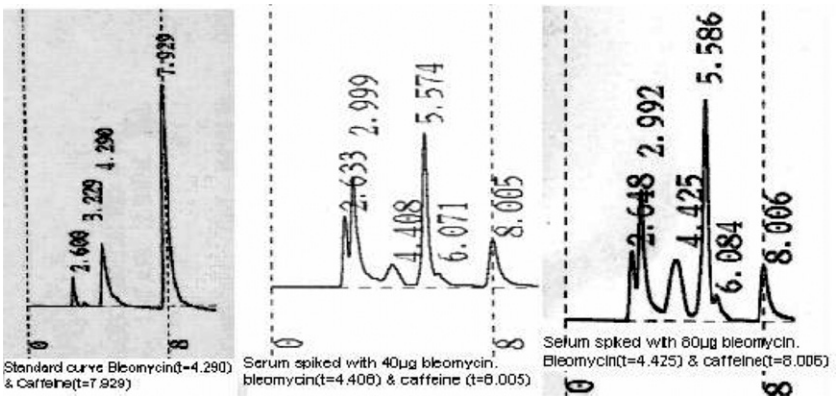

Fig. 3. Shows HPLC results of standard sample, 40 and 80 μg/ml spiked serum.

trols which were infused with 1 ml of bleomycin were collected as well.

2.7. High performance chromatography (HPLC) analysis

HPLC analysis was done using Agilent 1100LC equipped with a G1311A pump, DADG1315B variable wavelength UV–vis detector and a G1313A auto loop injector. The chromatograph column was a PLgel mixed-C column 300 mm × 7.5 mm while the aqueous column PL acquagel-OH mixed column 300 mm × 7.5 mm was used (Agilent techinologies). Trichloroacetic acid, EDTA–2Na, pure acetic acid, i.e. glacial acetic acid, methanol, acetonitrile, tetramethyl-ethylenediamine, caffeine and *N*-1-pentane sulfonic acid sodium salt monohydrate were all bought as reagent grade from Wako pure chemical industries.

The mobile phase consisted of 0.93 g of EDTA–2Na, 0.49 g of *N*-1-pentane sulfonic acid sodium salt monohydrate, 2.2 ml of tetramethyl-ethylenediamine, 4.5 ml pure acetic acid (all mixed in 500 ml of distilled water as a solvent):methanol:acetonitrile in a ratio of 74:18.6:7.4, respectively. The flow rate was 1 ml/min and the eluent was monitored spectometricaly at 40 °C, 291 nm, 0.04AUFS sensitivity. Caffeine was used as the internal standard. The above conditions were very similar to those used by Schilsky et al. (1993) and Aouida et al. (2004).

2.8. Solutions for external and internal standards

Two milligrams of bleomycin and 2.0 mg of caffeine were each dissolved in 10 ml of trichloroacetic acid and topped up with same to 200 μg/ml concentration and these were used as external and internal standards, respectively. Caffeine solution was further diluted to obtain 100 and 10 μg/ml while bleomycin solution was diluted to avail us with 160, 120, 80, 40, 20, 10 and 5 μg/ml. Rabbit serum spiked with bleomycin and caffeine at varying concentrations, i.e. 1600, 1200, 800, 400, 200, 100 and 50 μg/ml was obtained. Chromatography analysis of the above dilutions was done and standard curves obtained by plotting the ratio of peak area of bleomycin to internal standard (caffeine) versus concentration of bleomycin (Figs. 3 and 4).

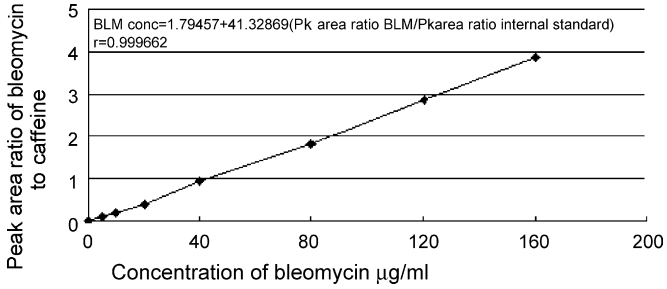

Fig. 4. Linear standard curve obtained by HPLC minimum concentration limit being 1 μg/ml.

2.9. Plasma and tissue drug concentration analysis

To each 400 μl of the obtained serum, homogenized tissue supernatant or standard sample, 40 μl of caffeine stock solution and 40 μl of 10% trichloroacetic acid were added then vortex mixed for 2 min before being centrifuged at 10,000 × *g* for 10 min. Twenty microliters aliquots of obtained supernatant was then injected into the chromatograph column and analyzed in triplicate. The concentrations of bleomycin were determined from peak area ratios of bleomycin against that of caffeine using the calibration graphs obtained earlier as a reference (using a least squares analysis of standard concentrations). Minimum detectable concentration was 1 μg/l.

2.10. Statistical analysis

With the help of PEMS3.0, Student's *t*-tests, regression and correlation analysis, Welch *t*-tests and other statistical tests were done as deemed necessary.

3. Results and discussion

3.1. Synthesis and characterization

The PVP based magnetic nanospheres were synthesized using gamma radiation and the characteristics are summarized in Table 1. There was good iron oxide distribution with in the nanospheres as seen in the TEM image (dark areas in micro-

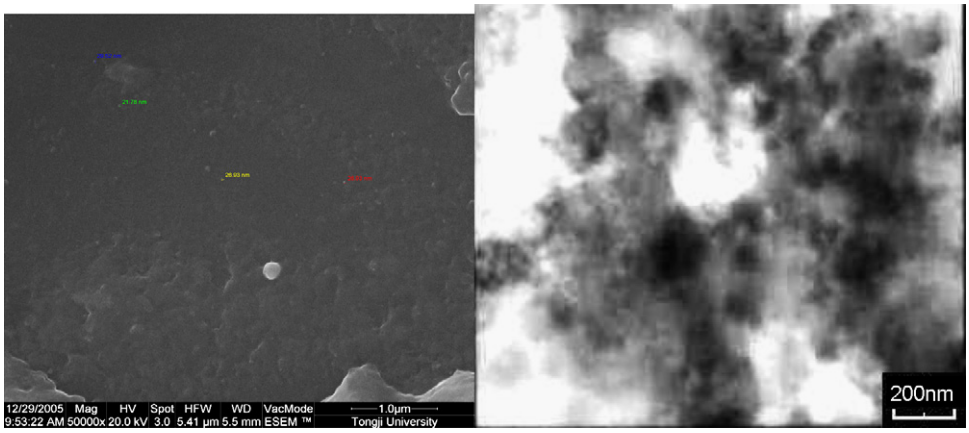

Fig. 5. ESEM and TEM images of the naonspheres. Note the colored spots in the ESEM image show the sizes of some stand alone nanospheres while the TEM show good iron oxide distribution.

graph). Just as reported by Pardoe et al. (2001) the iron particles tended to form necklace-like chains (image not shown). The average size was determined after the nanospheres were dispersed in normal saline with 10 min of sonication. They showed a tendency to aggregate. However some that stood as single nanospheres were measured using ESEM and ranged from 21.93 to 65.59 nm with a mean of 35.20 ± 15.29 nm. The TEM and ESEM images can be seen in Fig. 5. Aggregation of the ferrogel may be considered disadvantageous as it is expected to affect uptake by cells. However, research has shown that aggregation of some particles increases their accumulation in the solid tumor when compared to those with out that ability (Raucher and Chilkoti, 2001). We therefore feel that aggregation is an advantage since it allows the nanospheres to coalesce and block the arterioles and capillaries which not only reduces blood flow but also reduces the risk of stray particles. This is positive in that blood flow reduction results into more effective drug accumulation in addition to reduced tumor nutrient supply. However, aggregation may prove a hindrance in case of gene vector delivery hence requiring appropriate surface modification. Our aim in synthesizing this novel ferrogel was chemoembolization and therefore we expect this to generate further research in to other potential applications and hence required modifications. The variation in particle size could be controlled by use of techniques such as centrifugal fractionation and sieving. Further more the stirring speed and percentage of crosslinker have been shown to influence the size of the resultant particles for other carriers (Liu et al., 2005). Though not investigated in our study, we believe the same would apply and can be utilized to synthesize particles of bigger size. However it is worth noting that the changes in crosslinker percentage would also affect the swellability which in turn affects the drug absorption (Liu et al., 2005). Interestingly despite our particles being nano in size, the iron oxide content as determined by TG-DTA/DSC (Fig. 6) was very high at 70% (w/w). We therefore chose to use a 0.5 T magnet for our animals' experiments expecting it to provide sufficient magnetic attraction for the nanospheres to the tumor site. We considered it optimal since Goujun et al. had 33% iron content yet got good saturation magnetization (Liu et al., 2005). Fig. 7 shows the ferrogel attraction to a 0.5 T magnet applied to a plastic tube. The normal saline took about 3 min to fully become clear.

3.2. Biocompatibility studies

For any material to be considered in biomedical use, biocompatibility tests are a prerequisite. We carried out MTT tests, acute toxicity and in vitro hemolytic tests. The cell viability index of the MTT was calculated using the formula in Section 2 and then plotted against the extract dilutions. The results are shown in Fig. 8. From the figure it is seen that after both 24 and 72 h, there was varying degrees of toxicity. The lowest toxicity being seen in the 24 h group at 25% extracts concentration. The results go against the reported biocompatibility of PVP based

Table 1
characteristics of ferrofluid

Composition	Aqueous dispersion of PVP polymer magnetic microspheres
pH	7.4 ± 1
Particle size (mean)	35.20 ± 15.29 nm (21.93–65.59 nm)
PVP component	30%
Iron oxide component	70%
Odor	Odorless
Color	Brown
Nanospheres and drug stability	Atleast 1 month at −20 °C

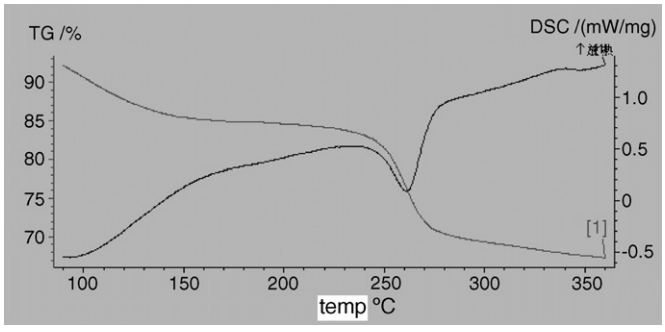

Fig. 6. TG-DTA/DSC results of the ferrofluid shows the PVP disintegration temperature was about 255 °C.

Fig. 7. Shows the attraction of the nanospheres to a 0.5 T magnet.

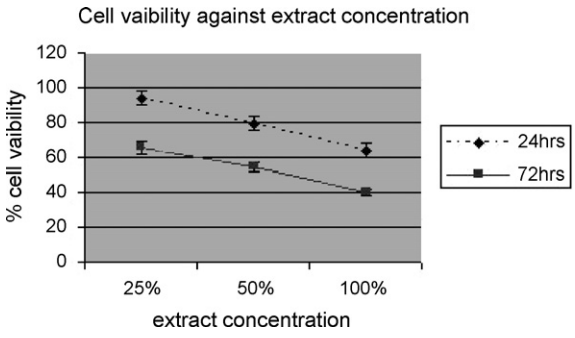

Fig. 8. Shows the cell viability index of extracts at given dilution after 24 and 72 h (MTT results).

products (Volker, 2004; Robinson et al., 1990). However when it comes to magnetic microparticles, MTT has been shown not to be reliable (Häfeli and Pauer, 1999). Therefore, the results are suspect and this may explain the apparent toxicity observed. In fact just like Häfeli, and Pauer, animal tests done by injecting extracts into rats did not show any observable signs of toxicity nor death for up to 1 month. However it is worth noting that Hong et al. (1996) reported cytostatic but not cytocidal effects of PVP based hydrogels which may explain to some extent the observed cell viability index. In Fig. 9, it can be noted that the cell morphology was not affected though when compared to the negative control, there was obviously less confluence which is in line with Hong et al.'s report. PVP is expected to be non-biodegradable (Robinson et al., 1990; Kodaira et al., 2004) and yet the differences between 24 and 72 h MTT results show some form of biodegradation. Hong et al. (1996) noted the presence of loose PVP particles in the rabbit retinas indicative of some form of biodegradation. It is therefore possible that the PVP magnetic nanospheres extract solutions under went some form of biodegradation releasing cytotoxic substances that affected the cells after 72 h. Factoring in Häfeli and Pauer (1999) and Hong et al. (1996), the MTT results obtained are undependable and thus more research is needed into biocompatibility, biodegradation and biodistribution of these nanospheres.

In vitro hemolytic index as calculated using a formula laid out in the methodology was $4.12 \pm 1.26\%$. Taking normal saline and distilled water as causing 0 and 100% hemolysis, respectively; we felt that the PVP magnetic nanospheres cause minimal hemolysis. It has been shown that PVP actually lowers hemolysis as a complex with some substances (Charvalos et al., 2006). Essentially we had expected no or negligible hemolysis. Hence there is need for further hemolytic tests including in vivo tests mimicking the anticipated application environment.

3.3. Drug release

In vitro release profile of bleomycin from the PVP hydrogel based magnetic nanospheres is as shown in Fig. 10. Bleomycin was quantitatively released with in slightly over 8 h from the nanospheres containing 1 mg bleomycin while the time was longer for those containing 3 and 5 mg. On the other hand free bleomycin quantitatively passed through the dialysis baffle with in only 3.5 h. While it took 2 h for 1, 3 and 5 mg of bound bleomycin to reach peak concentration, the free drug needed only 30 min. The rate of release of bound bleomycin is a good sign of reversibility of drug/hydrogel interaction a perquisite for magnetic microparticles drug delivery systems. The findings are consistent with reported release profiles of non-coupled/non-interacting drugs from PVP based hydrogels (Kaneda et al., 2004; Risbud et al., 2000; Charvalos et al., 2006).

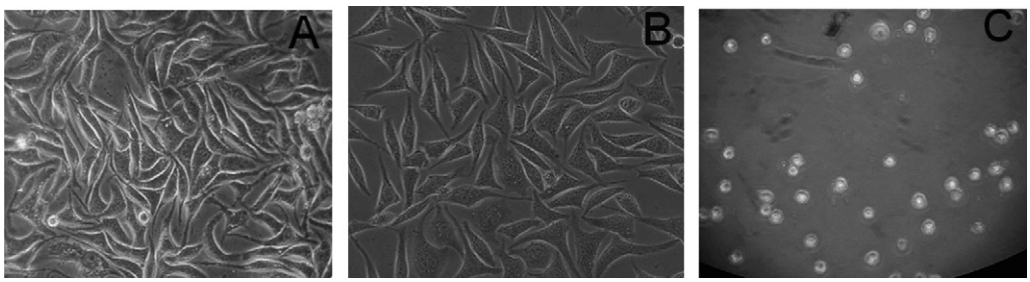

Fig. 9. Shows L929 cells morphology. (A) control with DMEM, (B) experimental with extract at 100% while (C) is the positive control (using latex extract) all taken after 24 h of culture.

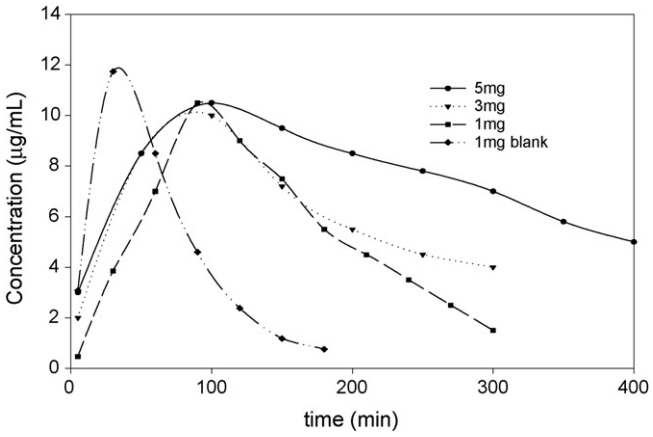

Fig. 10. In vitro drug release of free bleomycin versus ferrofluid bound bleomycin at 37 °C, pH 7.4. Three repeats all standard deviations were between 0.3 and 3 μg/ml.

The nanospheres therefore did not have covalent or ionic bonding with bleomycin.

Serum bleomycin concentration as a measure of in vivo drug release was monitored using HPLC and the results are as shown in Fig. 11. Both the control and experimental group, bleomycin was still traceable up to over 8 h. However the unbound drug peak concentration (20.87 ± 4.3 μg/ml) was attained only 30 min post infusion while that of the experimental group (7.32 ± 1.25 μg/ml) was reached after 60 min, i.e. twice the time. The peak concentration of the two groups was statistically significantly different ($p = 0.05$). The serum concentration of bleomycin from the free bleomycin (control) went down pretty fast falling to below 5 μg/ml with in 90 min while it took up to 360 min for that of the experimental group to reach the same level. The above observation implied need for a longer time lapse from infusion for bound bleomycin to reach given concentration and hence effective concentration compared to free drug. Under rather different experimental settings similar results have been reported demonstrating reduced pregnancy rate among rabbits that had delayed insemination as compared to the immediate group (Zavos et al., 1998). However, just as in the above reference after a given time interval the concentration of drug falls to ineffective levels. Therefore by studying the serum bleomycin

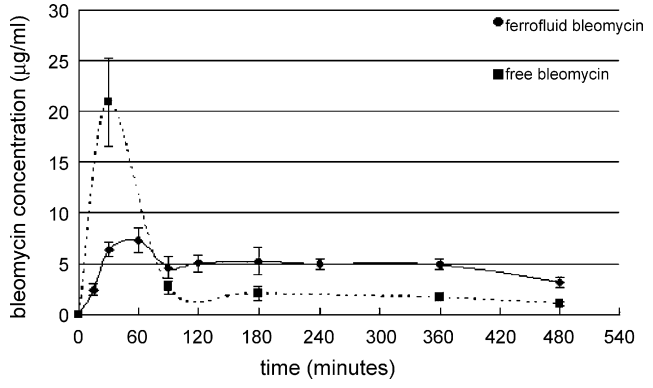

Fig. 11. In vivo drug release as monitored by instantaneous serum drug concentration using HPLC method. ($n = 5$ experimental group, $n = 5$ control group.)

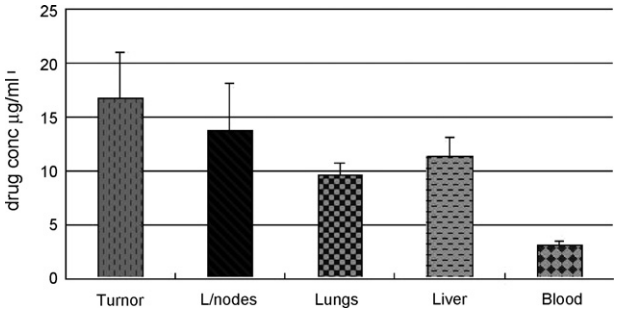

Fig. 12. The concentration of bleomycin in the experimental group tissues 8 h post infusion ($n = 5$).

concentration from the control and experimental group, dosage and regimen schedules need to be investigated further if effective chemotherapeutic drug levels are to be attained. We intend to do this by monitoring tumor size growth changes after infusion of the drug containing nanospheres.

Using HPLC the tissue bleomycin concentration from the experimental group was determined 8 h post infusion of the drug containing nanospheres and the results are shown in Fig. 11. The tumor had the highest concentration compared to all sampled tissues ($p = 0.05$). This is expected since bleomycin just like other antineoplastic drugs have an inherent physiological high affinity for malignancies due to the rate of cell division (Galmarini et al., 2003). Unfortunately due to enormous number of samples for HPLC and hence cost, we did not investigate tissue drug concentration for the control group. This would have gone along way in elucidating the role of our self-assembled PVP magnetic nanospheres in delivering and maintaining the tumor bleomycin concentration. The bleomycin concentration of the ipsilateral lymph nodes followed by liver, lung and blood in that order came in next ($p = 0.05$) (Fig. 12). The ipsilateral lymph nodes high concentration of bleomycin might be due to the inherent physiological selectivity of bleomycin to tumors since most of the parotid lymph nodes in our experimental animals had metastasis. However, the concentration of bleomycin in the liver, lung and blood 8 h post infusion of drug containing nanospheres, is different from that reported when ^{67}Ga–bleomycin complex in normal mice was investigated. In this research blood had higher radioactivity than either lungs or liver and likewise the lungs had more than the liver until 24 h post infusion with the status quo changing to the same order as we observed after 48 h post infusion (Faraj et al., 2003). We believe it would be interesting to see if the same would apply if we use mice under the same experimental conditions as in the reference above.

4. Conclusion

The present results indicate that PVP hydrogel based magnetic nanospheres as a potential drug carrier may have a future in magnetic guided chemotherapeutic drug delivery. They exhibited passive drug release that could be exploited to enhance therapeutic efficacy. The invivo drug circulation and concentration as determined by serum drug concentration was higher and maintained that level longer than the free bleomycin group

which is expected to affect efficacy. Therefore though more research needs to be done, we believe that PVP hydrogel magnetic nanospheres have potential and with further refinement could contribute towards magnetic drug guided delivery.

Acknowledgements

Financial support of the Shanghai local government scientific grants made the research possible. We also acknowledge the enormous work input by our colleagues in the basic science and pharmaceutical laboratory departments of Tongji hospital.

References

Anand, V.P., Cogdill, C.P., Klausner, K.A., Lister, L., Barbolt, T., Page, B.F., Urbanski, P., Woss, C.J., Boyce, J., 2003. Reevaluation of ethylene oxide hemolysis and irritation potential. J. Biomed. Mater. Res. A 15, 648–654.

Aouida, M., Leduc, A., Wang, H., Ramotar, D., 2004. Characterization of a transport and detoxification pathway for the antitumour drug bleomycin in *Saccharomyces cerevisiae*. Biochem. J. 15, 47–58.

Charvalos, E., Tzatzarakis, M.N., Van Bambeke, F., Tulkens, P.M., Tsatsakis, A.M., Tzanakakis, G.N., Mingeot-Leclercq, M.P., 2006. Water-soluble amphotericin B-polyvinylpyrrolidone complexes with maintained antifungal activity against *Candida* spp. and *Aspergillus* spp. and reduced haemolytic and cytotoxic effects. J. Antimicrob. Chemother. 57, 236–244.

Cheung, R.Y., Ying, Y., Rauth, A.M., Marcon, N., Yu Wu, X., 2005. Biodegradable dextran-based microspheres for delivery of anticancer drug mitomycin C. Biomaterials 26, 5375–5385.

Christoph, A., Wolfgang, A., Roswitha, J.K., Fritz, G.P., Peter, H., Christian, B., Wolfgang, E., Stefan, W., Andreas, S.L., 2000. Locoregional cancer treatment with magnetic drug targeting. Cancer Res. 60, 6641–6648.

Faraj, T., Bahram, B., Amir, R.J., Nariman, M., Hosein, R., Eisa, N.A., et al., 2003. Dynamic distribution of ^{67}Ga-bleomycin complex and carrier free ^{67}gallium in normal mice. IJPT 1, 24–29.

Galmarini, C.M., Jordheim, L., Dumontet, C., 2003. Pyrimidine nucleoside analogs in cancer treatment. Expert Rev. Anticancer Ther. 3, 717–728.

Gao, H., Wang, J.Y., Shen, X.Z., Deng, Y.H., Zhang, W., 2004. Preparation of magnetic polybutylcyanoacrylate nanospheres encapsulated with aclacinomycin A and its effect on gastric tumor. World J. Gastroenterol. 10, 2010–2013.

Gurnani, M., Lipari, P., Dell, J., Shi, B., Nielsen, L.L., 1999. Adenovirus-mediated p53 gene therapy has greater efficacy when combined with chemotherapy against human head and neck, ovarian, prostate, and breast cancer. Cancer Chemother. Pharmacol. 44, 143–151.

Häfeli, U.O., 2004. Magnetically modulated therapeutic systems. Int. J. Pharm. 277, 19–24.

Häfeli, U.O., Pauer, G.J, 1999. In vitro and in vivo toxicity of magnetic microspheres. J. Magn. Magn. Mater. 194, 76–82.

Hiroo, N., Takashi, S., Tadahiko, K., Shoji, S., Yuji, Y., Teruo, M., Mitsuo, O., 2004. Evaluation of systemic chemotherapy with magnetic liposomal doxorubicin and a dipole external electromagnet. Int. J. Cancer 109, 627–635.

Hong, Y., Chirila, T.V., Vijayasekaran, S., Dalton, P.D., Tahija, S.G., Cuypers, M.J., Constable, I.J., 1996. Crosslinked poly(1-vinyl-2-pyrrolidinone) as a vitreous substitute. J. Biomed. Mater. Res. 30, 441–448.

ISO document 10993, 1992. Biological compatibility of medical devices. Part 5. Tests for Cytotoxicity: In Vitro Methods.

Jana, S.S., Bharali, D.J., Mani, P., Maitra, A., Gupta, C.M., Sarkar, D.P., 2002. Targeted cytosolic delivery of hydrogel nanoparticles into HepG2 cells through engineered Sendai viral envelopes. FEBS Lett. 515, 184–188.

Kaneda, Y., Tsutsumi, Y., Yoshioka, Y., Kamada, H., Yamamoto, Y., Kodaira, H., Tsunoda, S., Okamoto, T., Mukai, Y., Shibata, H., Nakagawa, S., Mayumi, T., 2004. The use of PVP as a polymeric carrier to improve the plasma half-life of drugs. Biomaterials 25, 3259–3266.

Kodaira, H., Tsutsumi, Y., Yoshioka, Y., Kamada, H., Kaneda, Y., Yamamoto, Y., Tsunoda, S., et al., 2004. The targeting of anionized polyvinylpyrrolidone to the renal system. Biomaterials 25, 4309–4315.

Kupsch, P., Henning, B.F., Passarge, K., Richly, H., Wiesemann, K., Hilger, R.A., et al., 2005. Results of a phase I trial of sorafenib (BAY 43-9006) in combination with oxaliplatin in patients with refractory solid tumors, including colorectal cancer. Clin. Colorectal Cancer 5, 188–196.

Liu, G., Yang, H., Zhou, J., Law, S.J., Jiang, Q., Yang, G., 2005. Preparation of magnetic microspheres from water-in-oil emulsion stabilized by block copolymer dispersant. Biomacromolecules 6, 1280–1288.

Lubbe, A.S., Alexiou, C., Bergemann, C., 2001. Clinical applications of magnetic drug targeting. J. Surg. Res. 95, 200–206.

Lubbe, A.S., Bergemann, C., Huhnt, W., Fricke, T., Riess, H., Brock, J.W., Huhn, D., 1996a. Preclinical experiences with magnetic drug targeting: tolerance and efficacy. Cancer Res. 56, 4694–4701.

Lubbe, A.S., Bergemann, C., Riess, H., Schriever, F., Reichardt, P., Possinger, K., Matthias, M., Dorken, B., Herrmann, F., Gurtler, R., Hohenberger, P., Haas, N., Sohr, R., Sander, B., Lemke, A.J., Ohlendorf, D., Huhnt, W., Huhn, D., 1996b. Clinical experiences with magnetic drug targeting: a phase I study with 4′-epidoxorubicin in 14 patients with advanced solid tumors. Cancer Res. 56, 4686–4693.

Müler, R.H., Mssβen, S., Weyhers, H., 1996. Cytotoxicity of magnetite-loaded polylactide, polylactide/glycolide and solid lipid nanoparticles. Int. J. Pharm. 138, 85–94.

Pardoe, H., Chua-anusorn, W., St. Pierre, T.G., Dobson, J., 2001. Structural and magnetic properties of nanoscale iron oxide particles synthesized in the presence of dextran and polyvinyl alcohol. J. Magn. Magn. Mater. 225, 41–46.

Raucher, D., Chilkoti, A., 2001. Enhanced uptake of a thermally responsive polypeptide by tumor cells in response to its hyperthermia-mediated phase transition. Cancer Res. 61, 7163–7170.

Reimer, K., Fleischer, W., Brogmann, B., Schreier, H., Burkhard, P., Lanzendorfer, A., Gumbel, H., Hoekstra, H., Behrens-Baumann, W., 1997. Povidone–iodine liposomes—an overview. Dermatology 195, 93–99.

Risbud, M.V., Hardikar, A.A., Bhat, S.V., Bhonde, R.R., 2000. pH-sensitive freeze-dried chitosan-polyvinyl pyrrolidone hydrogels as controlled release system for antibiotic delivery. J. Control. Release. 68, 23–30.

Robinson, B.V., Sullivan, F.M., Borzelleca, J.F., Schwartz, S.L., 1990. A critical review of kinetics and toxicology of polyvinylpyrrolidone (Povidone). Lewis publishers, Inc., Chelsea, MI.

Rudge, S., Peterson, C., Vessely, C., Koda, J., Stevens, S., Catterall, L., 2001. Adsorption and desorption of chemotherapeutic drugs from a magnetically targeted carrier (MTC). J. Control. Release. 74, 335–340.

Schilsky, R.L., Janisch, L., Berezin, B., Mick, R., Vogelzang, N.J., Ratain, M.J., 1993. Phase I clinical and pharmacological study of iododeoxyuridine and bleomycin in patients with advnced cancer. Cancer Res. 53, 1293–1296.

Tapan, K.J., Marco, A.M., Sanjeeb, K.S., Leslie-Pelecky, D.L., Vinod, L., 2005. Iron oxide nanoparticles for sustained delivery of anticancer agents. Mol. Pharm. 2, 194–205.

Volker, B., 2004. Polyvinylpyrrolidone Excipients for Pharmaceuticals: Povidone, Crospovidone and Copovidone. Springer-Verlag and Heidelberg GmbH & Co., Berlin and UK.

Yong, J.I.N., Jun, L.I., Long-fu, R., Xiong-wen LÜ, Yan, H., Shu-yun, XU, 2005. Pharmacokinetics and tissue distribution of 5-fluorouracil encapsulated by galactosylceramide liposomes in mice. Acta Pharm. Sin. 26, 250–256.

Youssef, J., David, J.W., 2000. Combination of the bioreductive drug tirapazamine with the chemotherapeutic prodrug cyclophosphamide for P450/P450-reductase-based cancer gene therapy. Cancer Res. 60, 3761–3769.

Zavos, P.M., Correa, J.R., Zarmakoupis-Zavos, P.N., 1998. Assessment of a tablet drug delivery system incorporating nonoxynol-9 co-precipitated with polyvinylpyrrolidone in preventing the onset of pregnancy in rabbits. Fertil. Steril. 69, 768–773.